



Systemic Mesenchymal Stromal Cell Transplantation Prevents Functional Bone Loss in a Mouse Model of Age-Related Osteoporosis

JEFFREY KIERNAN,^a SALLY HU,^b MARC D. GRYPAS,^{b,c} JOHN E. DAVIES,^{a,d} WILLIAM L. STANFORD^{a,e,f}

Key Words. Mesenchymal stem cell • Tissue-specific stem cells • Stem cell transplantation • Osteoporosis • Sca-1

ABSTRACT

Age-related osteoporosis is driven by defects in the tissue-resident mesenchymal stromal cells (MSCs), a heterogeneous population of musculoskeletal progenitors that includes skeletal stem cells. MSC decline leads to reduced bone formation, causing loss of bone volume and the breakdown of bony microarchitecture crucial to trabecular strength. Furthermore, the low-turnover state precipitated by MSC loss leads to low-quality bone that is unable to perform remodeling-mediated maintenance—replacing old damaged bone with new healthy tissue. Using minimally expanded exogenous MSCs injected systemically into a mouse model of human age-related osteoporosis, we show long-term engraftment and markedly increased bone formation. This led to improved bone quality and turnover and, importantly, sustained microarchitectural competence. These data establish proof of concept that MSC transplantation may be used to prevent or treat human age-related osteoporosis. *STEM CELLS TRANSLATIONAL MEDICINE* 2016;5:683–693

SIGNIFICANCE

This study shows that a single dose of minimally expanded mesenchymal stromal cells (MSCs) injected systemically into a mouse model of human age-related osteoporosis display long-term engraftment and prevent the decline in bone formation, bone quality, and microarchitectural competence. This work adds to a growing body of evidence suggesting that the decline of MSCs associated with age-related osteoporosis is a major transformative event in the progression of the disease. Furthermore, it establishes proof of concept that MSC transplantation may be a viable therapeutic strategy to treat or prevent human age-related osteoporosis.

INTRODUCTION

Almost a century ago, the axiom “form follows function” was established by the seminal treatise of D’Arcy Thompson, who compared, predominantly, hard tissue structures across phyla [1]. The anisotropy and connectivity of trabecular bone, and their loss in certain pathologies, are prime examples of this axiom [1, 2] and are known to affect the mechanical performance of bone tissue [2–4]. Thus, the regeneration of such an important structural tissue should aim not only to create new tissue, but also to recapitulate its functional, anisotropic, interconnected microstructure. It is surprising, therefore, that current therapeutic strategies, from bone-substitute biomaterials to stem cell transplantation, have paid little heed to the form and function of the regenerated tissue.

Bone is a dynamic tissue, with remodeling-mediated maintenance regenerating the entire skeleton every 10 years [5]. Bone formation and

resorption are tightly coupled in this process, and any imbalance can manifest itself in osteoporosis, a disease representing significant morbidity and substantial health care burden [6]. Age-related (type II, senile) osteoporosis presents a bone formation deficit caused by age-related changes in the proliferation and differentiation capacity of mesenchymal stromal cells (MSCs) [7, 8]. The resultant uncoupling of remodeling-mediated maintenance leads to a low-turnover osteoporotic state and facilitates mechanical weakness due to loss of bone volume and microarchitectural integrity, combined with the presence of old, hypermineralized, damaged bone [9].

MSCs and the rare skeletal stem cells (SSCs) present within this population hold significant therapeutic potential, directly by mediating tissue repair through differentiation into various musculoskeletal tissues [10], or indirectly by secreting a myriad of growth factors and immunomodulatory

^aInstitute of Biomaterials and Biomedical Engineering, ^bDepartment of Laboratory Medicine and Pathobiology, and ^dFaculty of Dentistry, University of Toronto, Toronto, Ontario, Canada; ^cLunenfeld-Tanenbaum Research Institute, Mount Sinai Hospital, Toronto, Ontario, Canada; ^eSprott Centre for Stem Cell Research, Ottawa Hospital Research Institute, Ottawa, Ontario, Canada; ^fDepartment of Cellular and Molecular Medicine and Department of Biochemistry, Microbiology, and Immunology, University of Ottawa, Ottawa, Ontario, Canada

Correspondence: William L. Stanford, Ph.D., Ottawa Hospital Research Institute, Ottawa Hospital, 501 Smyth Road, Box 511, Ottawa, Ontario K1H 8L6, Canada. Telephone: 613-737-8899, ext. 73841; E-Mail: wstanford@ohri.ca; or John E. Davies, Ph.D., D.Sc., Institute of Biomaterials and Biomedical Engineering, Rosebrugh Building, Room 407, 164 College Street, Toronto, Ontario M5S 3G9, Canada. Telephone: 416-978-1471; E-Mail: jed.davies@utoronto.ca

Received September 3, 2015; accepted for publication November 23, 2015; published Online First on March 17, 2016.

©AlphaMed Press
1066-5099/2016/\$20.00/0

<http://dx.doi.org/10.5966/sctm.2015-0231>

cytokines [11]. To date, more than 500 clinical trials using MSCs have been registered with clinicaltrials.gov, with some trials showing significant benefit toward treating bone-related conditions [12]. One particular study used intravenous delivery of MSCs to treat children with osteogenesis imperfecta, demonstrating an encouraging short-term therapeutic effect [13]. However, early ambiguities in the identity of MSCs may have contributed to the lack of long-term effect [14]. Recent breakthroughs elucidating the hierarchy of musculoskeletal progenitors, particularly the characterization of SSCs [15–18], will likely improve the clinical outcome of future MSC therapy trials.

Osteoporosis could benefit from MSC therapy, particularly because MSC depletion drives disease progression; however, no clinical trials are currently underway or recruiting to assess the therapeutic potential of MSCs to treat osteoporosis. Because of poor homing abilities of culture expanded MSC to bone [19–21], existing animal studies using MSCs to increase bone formation have relied on local administration of MSCs [22], genetic manipulation [23], or surface modification [21, 24].

Sca-1 null (*Sca-1*^{-/-}) mice demonstrate a cell autonomous deficiency in the ability of MSC to support bone formation, facilitating a low-turnover state with progressive bone loss and mechanical weakness beyond 6 months of age. As such, osteopenia observed in *Sca-1*^{-/-} mice is considered a model of human type II osteoporosis [25, 26]. These findings suggested that MSCs could be used as a therapeutic target or cell-based therapy to treat age-related osteoporosis. As a first step toward testing this hypothesis, we sought to determine whether minimally expanded MSCs can engraft long-term in vivo and prevent the onset of osteopenia in *Sca-1*^{-/-} mice. Indeed, we now demonstrate that a single bolus of minimally expanded, wild-type (WT), donor MSCs prevents the decline of bone formation, markedly increases bone turnover, and results in the long-term maintenance of trabecular architectural anisotropy and connectivity. Because osteoporosis in humans is associated with a decrease in these microarchitectural features that lead to increased fracture risk [27], our findings suggest that such MSC therapy may lead to broad and long-term regenerative consequences that address both the form and function of bone. Furthermore, this work demonstrates the therapeutic promise of minimally expanded MSC populations.

MATERIALS AND METHODS

Study Design

This controlled laboratory experiment was undertaken to assess the therapeutic potential of MSCs to treat progressive age-dependent bone loss in our *Sca-1*^{-/-} model of human age-related osteoporosis. All experiments were carried out in age-matched *Sca-1*^{-/-} or WT mice, with a majority of analysis focusing on cell engraftment and functional recovery of bone quality. Sample size was chosen for consistency with previous investigations of the *Sca-1*^{-/-} phenotype [25, 26], and outliers (data points more than 2 standard deviations above or below the mean) were removed from the statistical analysis. Multiple donor-cell isolation procedures were carried out, and multiple litters of WT and *Sca-1*^{-/-} mice were used for transplantation and control cohorts for this study. This study was not blinded; laboratory standard operating procedures were used for analysis, and specialized, automated image analysis software (Bioquant, Nashville, TN, <http://www.bioquant.com>) was used for consistent and unbiased data.

MSC Isolation and Transplant

The MSC isolation protocol was modified from that of StemCell Technologies (Vancouver, BC, Canada, <http://www.stemcell.com>). The 5- to 6-month-old male WT or *C.FVB-Tg(CAG-luc, GFP)L2G85Chco/FathJ* (or *GFP-LUC*) mice were euthanized by isoflurane overdose and sprayed with 70% ethanol. Workflow is outlined in Figure 1A. Hind legs were removed and placed on ice. Bones from the iliac crest, femur, and tibia were removed, and muscle tissue was removed. Bones from three or four mice were pooled together in a mortar with 5–7 ml of buffer (PBS with 2% FBS plus 1 mM EDTA). Bones were crushed with a pestle to release marrow. Marrow was reserved at room temperature, while bone fragments were cut into small fragments, placed into a 50-ml conical tube, and digested in 0.25% type I collagenase (StemCell Technologies) for 45 minutes in a shaking incubator at 37°C and 160 rpm. This solution was then mixed with the bone marrow, and passage 0 (P0) cells were plated in 10-cm tissue culture dishes at a density of 333,333 per cm² in MSC medium consisting of 80% Minimum Essential Medium (MEM) Alpha (ThermoFisher Scientific, Oakwood Village, OH, <https://www.thermofisher.com>), 20% mouse MSC stimulatory supplements (StemCell Technologies), and 50 U/ml penicillin and 50 µg/ml streptomycin (ThermoFisher Scientific). Medium was changed every 3 days, and cells were grown until 70%–80% confluent (7–10 days). P0 cells were harvested by adding 0.25% trypsin-EDTA (ThermoFisher Scientific catalog number 25200056) for 5 minutes, and any cells remaining on the plate were discarded. To remove hematopoietic contamination, harvested P0 cells were stained with purified rat anti-mouse antibodies against hematopoietic cell markers CD45 (clone number 30-F11, eBioscience, San Diego, CA, <http://www.ebioscience.com>) and CD11b (clone number M1/70, eBioscience) at a concentration of 1:167, followed by incubation with immunomagnetic sheep anti-rat IgG antibody (ThermoFisher Scientific) as per manufacturer's instructions, and magnetic depletion was performed to remove cells conjugated to iron antibodies. Remaining nonhematopoietic cells were replated as passage 1 (P1) MSCs in MSC medium at a density of 5,000 cells per cm². P1 MSCs were grown for 3–4 days until cells were approximately 60%–70% confluent. At this point, MSCs were harvested with 2 ml of 0.25% trypsin-EDTA, washed twice in PBS (without MgCl₂ or CaCl₂), and suspended at a concentration of 2.0 × 10⁷ cells per ml. In all cases, mice received 2.0 × 10⁶ (except 4.0 × 10⁶ cells in one set of experiments; Fig. 2) MSCs in a total volume of 100 µl via tail vein injection.

To harvest cells from recipient mice for the short-term studies, marrow was flushed with a 23-gauge needle, and compact bone cells were isolated by crushing flushed bone and digesting with 0.25% type I collagenase solution (StemCell Technologies). Red blood cells were lysed with red cell lysis buffer. For long-term engraftment studies, bone marrow and compact bone cells harvested from recipient mice for analysis occurred in the same manner as in the preceding process up until the point of antibody staining with the following modifications. Cells were isolated from individual mice with separate mortars and pestles, and red blood cells were lysed with red cell lysis buffer.

Multispectral In Vivo/Ex Vivo Imaging

Mice were anesthetized, depleted, and transferred to a Kodak In Vivo Multispectral Imaging System (Carestream Health, Rochester, NY,

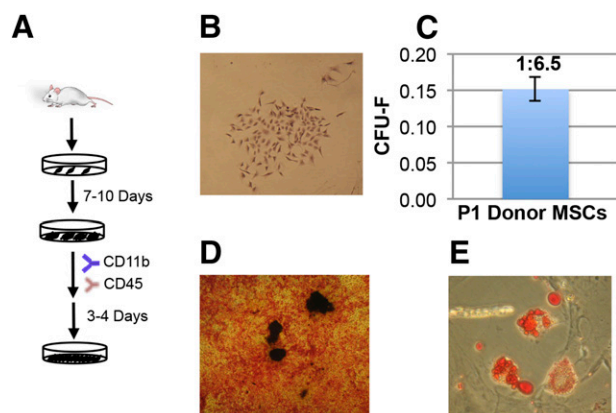


Figure 1. Isolation and differentiation capacity of donor MSCs. **(A):** A workflow diagram showing WT MSC isolation. **(B):** Single cell derived colony derived from passage 1 donor MSCs ($\times 4$ magnification, Crystal Violet stain). **(C):** Passage 1 donor MSCs had a CFU-F frequency of 1:6.5 ($n = 3$). **(D):** Passage 1 donor MSCs grown under osteogenic conditions form bone nodules ($\times 4$ magnification, Von Kossa stain). **(E):** Passage 1 donor MSCs grown under adipogenic conditions form adipocytes ($\times 10$ magnification, Oil Red O stain). Abbreviations: CFU-F, colony-forming unit fibroblast; MSCs, mesenchymal stromal cells; P1, passage 1; WT, wild type.

<http://www.carestream.com>). Fluorescence measurements of 1,1'-diocadecyl-3,3',3'-tetramethylindotricarbocyanine iodide (DiR; ThermoFisher Scientific; 750/830 nm) were acquired for 5 minutes, x-ray images were acquired for 2.5 minutes, and color images were acquired by using a 1-second exposure. Animals were then euthanized by isoflurane overdose, and organs and bones were harvested and underwent ex vivo imaging (same as in vivo). Unmixed 16-bit images were background-subtracted in ImageJ. Pixel intensity measurements were obtained from the region of interest (ROI) (proximal tibia/distal femur or harvested organs) and used to determine mean pixel intensity.

Statistical Analysis

For all statistical analysis, one-way analysis of variance was performed to assess significant differences across groups. If a significant difference was present, a Bonferroni post hoc test was used for pairwise comparisons. Data points that were more than 2 standard deviations above or below the mean were considered outliers.

Additional materials and methods can be found in the supplemental online data.

RESULTS

Isolation and Characterization of Donor MSC Population

The cell source is a critical consideration for the development of cell-based therapies. We reasoned that a population enriched for clonogenic MSCs would be osteogenic and capable of maintaining bone homeostasis for long periods. A highly clonogenic donor MSC population was isolated as previously described [28]. We empirically developed a standard procedure based on optimized plating density, length of trypsinization, and immunodepletion of hematopoietic cells (Fig. 1A). This approach consistently yielded a MSC population capable of generating

single cell-derived colonies (Fig. 1B) and retained a high colony-forming unit fibroblast frequency of approximately 1:6.5 (Fig. 1C). These minimally expanded MSCs were capable of osteogenic differentiation, robustly forming bone nodules (brown bone surrounded by pink alkaline phosphatase-stained cells) (Fig. 1D), with a colony-forming unit osteoblast frequency of approximately 1:1,300. MSCs were also capable of adipogenic differentiation, forming adipocytes that exhibit oil red O staining of fat deposits (Fig. 1E). Passage 1 MSCs express Sca-1, CD44, CD106, and CD29, markers common to murine MSCs, and are absent for hematopoietic markers CD45 and CD11b (supplemental online Fig. 1).

Donor MSCs Are Capable of Delivery to the Long Bones of Recipient Mice

Short-term homing studies were performed to investigate whether minimally expanded MSCs could migrate to, and lodge in, the bone marrow of the *Sca-1*^{-/-} mouse. Recipient mice did not undergo myeloablative conditioning because this has been shown to be injurious to local MSCs [29], and future clinical adaptation of the protocol would prohibit such conditioning in elderly humans. Before transplantation, donor cells were labeled with near-IR lipophilic carbocyanine dye DiR, and either 2×10^6 or 4×10^6 cells were injected into the tail vein. Mice were subjected to in vivo imaging at 24 and 48 hours after injection, followed by euthanasia and dissection of organs and bones that were subsequently imaged ex vivo. Transplanted WT MSCs were detected in the long bones (tibia and femur) of *Sca-1*^{-/-} mice and were maintained for a period of at least 48 hours (Fig. 2A, 2B). The majority of donor signal was found in the lungs, liver, and spleen of recipient mice (Fig. 2A, 2B). No DiR signal was detected in naïve *Sca-1*^{-/-} mice (Fig. 2A, 2B). Fluorescence was also observed in the tail at the injection site because of unavoidable donor cell contact with surrounding tissue. Mice that received the higher cell dose demonstrated a greater DiR signal at the proximal tibia/distal femur site in vivo (supplemental online Fig. 2A) and in visceral organs and long bones ex vivo (supplemental online Fig. 2B). Significantly, transplanted MSCs displayed dose-dependent delivery to the long bones of recipient mice.

Donor MSCs Are Capable of Short-Term Residence Within the Bone Marrow

We tracked WT MSCs for 2 weeks after transplantation to discern whether cells were maintained within the bone marrow of treated mice. Mice were injected with 2×10^6 DiR-labeled WT MSCs, followed by euthanasia and ex vivo imaging of dissected bones at 1, 7, and 14 days after transplantation. After imaging, the bone marrow was flushed, and cytometric analysis was performed. No DiR fluorescence was detected in the bones or bone marrow cells of naïve *Sca-1*^{-/-} mice at day 1, 7, and 14, whereas DiR⁺ cells were detected in *Sca-1*^{-/-} mice receiving WT MSC transplant (supplemental online Fig. 3A, 3B). The average DiR fluorescence intensity of whole bones decreased with time, and was consistent with a declining number of engrafted MSCs assessed (supplemental online Fig. 3A, 3B). To investigate the location of the transplanted cells within the bone, *Sca-1*^{-/-} mice were transplanted as described above and assessed 2 weeks later. The mean pixel intensity was

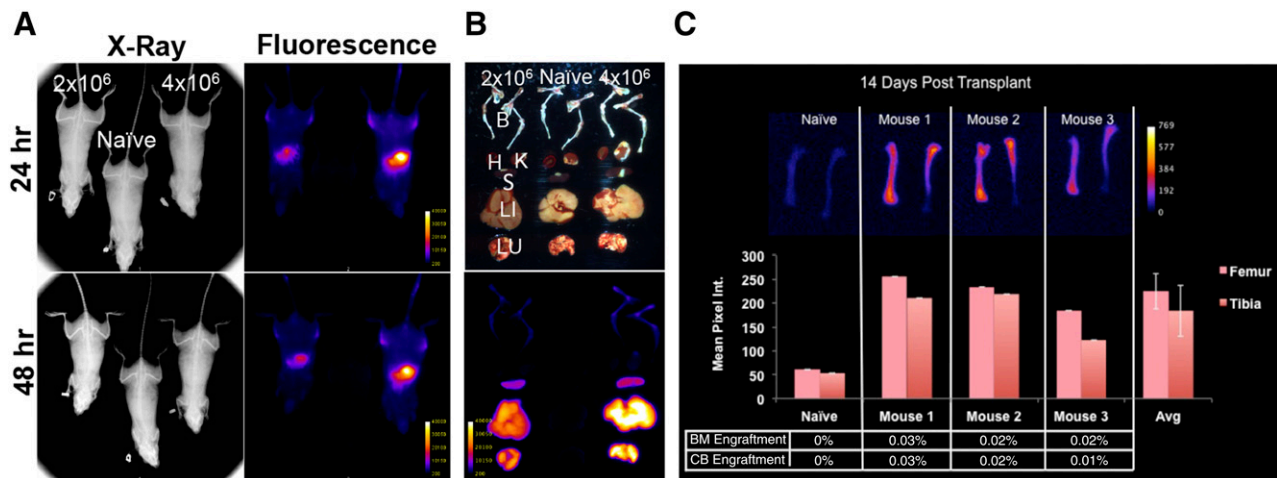


Figure 2. Short-term analysis confirms systemically injected purified MSCs are delivered and retained in the bone marrow, lungs, and liver. **(A):** In vivo fluorescent imaging (top) and x-ray (bottom) of untreated naïve and DiR⁺ MSC-transplanted *Sca-1*^{-/-} mice. **(B):** Ex vivo fluorescent imaging of organs/bones, color (top) and fluorescence (bottom). **(C):** DiR fluorescence present in bones 2 weeks after DiR⁺ MSC transplant in *Sca-1*^{-/-} mice compared with naïve *Sca-1*^{-/-} mice and percent presence of DiR-labeled cells in the BM and CB assessed via flow cytometry ($n = 3$). Abbreviations: Avg, average; B, bones; BM, bone marrow; CB, compact bone; DiR, 1,1'-dioctadecyl-3,3,3',3'-tetramethylindotricarbocyanine iodide; H, heart; K, kidney; Li, liver; Lu, lungs; MSCs, mesenchymal stromal cells; S, spleen.

measured in the femurs and tibias of three treated mice, along with naïve *Sca-1*^{-/-} controls, followed by isolation of bone marrow and compact bone cells separately. Similar DiR fluorescence was present in femurs and tibias of individual MSC-transplanted mice (Fig. 2C). Consistent with this finding, cytometric analyses demonstrated evenly distributed donor cell residence within the bone marrow and compact bone of individual mice.

Transplanted MSCs Are Capable of Long-Term Engraftment

GFP-LUC mice were used to track long-term MSC engraftment. This dual reporter transgenic mouse is on the same genetic background as the *Sca-1*^{-/-} mice used here (*BALB/c*) and expresses luciferase and GFP. Low-level GFP expression is present in the MSC population [30] and absent in hematopoietic cells [31]. Male mice were chosen as donors to allow the use of Y-chromosome quantitative polymerase chain reaction (qPCR) in female recipients as an additional marker. Consistent with published strain data, very few GFP-positive cells were identified in the bone marrow and compact bone harvested from *GFP-LUC* mice (Fig. 3A). Significantly, when this fraction was plated and adherent cells grown to 60%–70% confluence (passage 0), GFP fluorescence was detected in 40%–50% of cells (Fig. 3B). Adherent cells were passaged, and hematopoietic cells magnetically depleted (Fig. 1A), before being replated and again grown to 70% confluence. These passage 1 MSCs expressed low levels of GFP (Fig. 3B) and were used as the donor cell population for the long-term transplantation experiments.

The 10-week-old *Sca-1*^{-/-} mice were transplanted with 2×10^6 *GFP-LUC* MSCs and assessed 24 weeks later. Mice were analyzed for GFP expression and Y-chromosome presence by flow cytometry and Taqman qPCR, respectively. Cells were harvested as outlined in Figure 1A and stained with purified rat antibodies against hematopoietic markers CD45, CD11b, and Ter119 endothelial marker CD31, followed by iron-conjugated sheep anti-rat antibodies facilitating magnetic immunodepletion of non-MSCs. The remaining 2% of enriched cells not expressing

hematopoietic or endothelial markers (data not shown) were analyzed for GFP expression versus near-IR dead cell exclusion. In the positive control *GFP-LUC* donor mice, only 0.06% of enriched cells expressed detectable GFP (Fig. 3C). A low frequency (0.002%–0.003%) of enriched cells recovered from some *Sca-1*^{-/-} mice that received an MSC transplant expressed detectable GFP signal. However, upon normalization to GFP⁺ cells present in the same cell fraction of *GFP-LUC* mice, these numbers represent 3%–5% engraftment (Fig. 3D, 3E). No GFP signal was detected in naïve *Sca-1*^{-/-} mice (Fig. 3F).

To confirm these findings, genomic DNA was isolated from the enriched cell population and analyzed by Taqman qPCR detection of the donor male Y-chromosome presence. Donor engraftment of 0.0005%–0.02% was present in the enriched cell fraction (Fig. 3G and supplemental online Fig. 4A). The enriched cell population represented approximately 2% of total cells harvested from the bone marrow and compact bone. Therefore, donor contribution of 0.00001% and 0.0005% within the total cell population was observed (Fig. 3G). Mouse MSCs are extremely rare in situ and comprise only 0.0003% of cells in the bone marrow, which equates to 3 cells per million [32]. Donor MSC contribution represented significant engraftment of between 4 and 224 cells per million of the enriched cell fraction and 0.1 and 4.5 cells per million of total bone cells (Fig. 3G). Long-term engraftment was detected in 5 of 15 recipient mice, although levels below the detection limit could have been present. Significantly higher engraftment was revealed in the lungs of all recipient mice analyzed, with an average engraftment of 0.23%, or 2,300 cells per million of total lung cells (Fig. 3G), proportionate to the large numbers of transplanted cells detected in the lungs within 48 hours of transplantation. No engraftment was identified in the liver of recipient animals (Fig. 3G).

A previous study documented upregulation of monocyte colony stimulating factor 1 (M-CSF) expression in lung-entrapped MSCs [33]. As M-CSF is a cytokine required for osteoclast formation, we tested whether elevated M-CSF levels were present in the serum of transplanted animals. However, no difference in M-CSF between MSC-transplanted and naïve *Sca-1*^{-/-} control

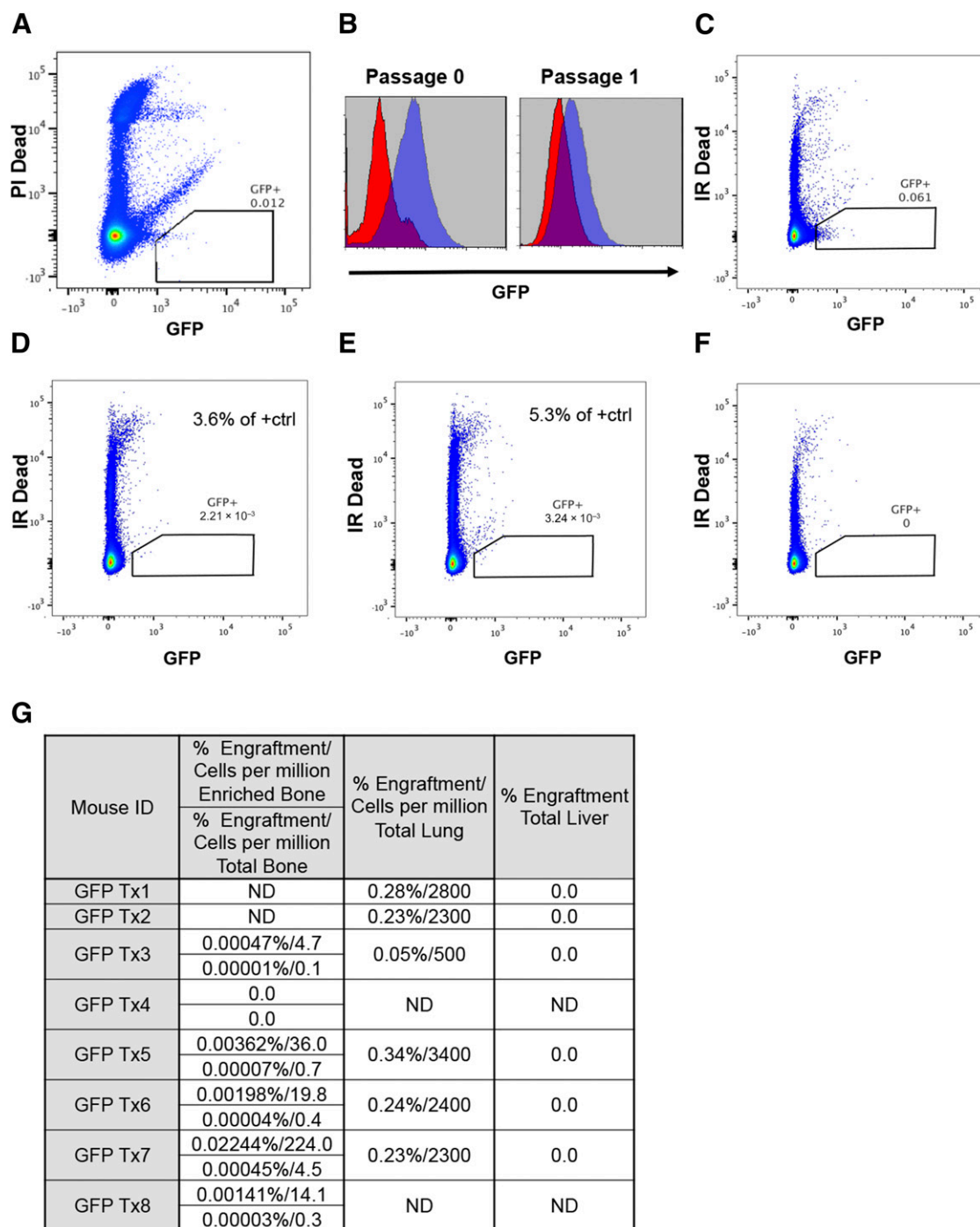


Figure 3. Transplanted GFP⁺ MSCs are capable of persistent engraftment in the marrow/endosteal region of *Sca-1*^{-/-} for 6 months. **(A–F):** Flow cytometric analysis. **(A):** GFP signal of total bone marrow/compact bone cells from donor *GFP-LUC* mice. **(B):** GFP signal of donor MSCs at passage 0 and 1. **(C):** GFP signal of enriched cells from donor *GFP-LUC* mice. **(D, E):** Two examples of mice that displayed GFP⁺ cells. **(F):** GFP signal was absent from naïve *Sca-1*^{-/-} mice. **(G):** Table displaying quantitative polymerase chain reaction detection of Y-chromosome engraftment; percent donor engraftment and engrafted cells per million of enriched nonhematopoietic/nonendothelial fraction of bone marrow/compact bone cells, percent donor engraftment, and cells per million in total nucleated bone marrow cells; percent donor engraftment and cells per million of total lung cells; and percent donor engraftment in total liver cells. Abbreviations: ctrl, control; GFP, green fluorescent protein; LUC, luciferase; MSCs, mesenchymal stromal cells; ND, not determined; PI, propidium iodide.

mice was detected (data not shown). Along with M-CSF, Receptor Activator of Nuclear Factor κ -B Ligand (RANKL) is required for osteoclast differentiation and is primarily produced by osteoblasts and osteocytes. Thus, we assessed whether RANKL levels were

elevated in the serum of transplanted animals. Similar to M-CSF levels, no significant difference in RANKL levels between MSC-transplanted and naïve *Sca-1*^{-/-} control mice was detected (data not shown).

Transplanted *Sca-1*^{-/-} Mice Displayed Improved Trabecular Bone Formation, Bone Turnover, and Osteoclast Frequency

Previously, we demonstrated that *Sca-1*^{-/-} mice have reduced active bone formation during aging, driven by defective self-renewal of MSCs and associated reduction in osteoblasts [25]. Deficiencies in bone formation are likewise present in human aging and clinical osteoporosis [34, 35]. We tested whether a single, systemic dose of WT MSCs into *Sca-1*^{-/-} mice could prevent the bone deterioration observed by 6 months of age. *Sca-1*^{-/-} mice were transplanted as described above, and 24 weeks later, at 10 and 2 days before euthanasia, mice were injected with calcein green, a fluorescent marker of bone formation. WT mice displayed greater bone formation, observed by bright green calcein labeling in trabecular tissue of the proximal tibia, than MSC-transplanted mice, which themselves showed more formation than naïve *Sca-1*^{-/-} mice (Fig. 4A). Quantitatively, naïve *Sca-1*^{-/-} mice exhibited a significantly reduced area undergoing active bone formation compared with WT mice, as indicated by mineralizing surface area normalized to total bone surface area (MS/BS). Significantly more area of active bone formation occurred in MSC-transplanted *Sca-1*^{-/-} mice, with MS/BS nearly equaling that of WT mice (Fig. 4B).

We further analyzed calcein integration to elucidate whether the actual rate of bone formation was impaired in *Sca-1*^{-/-} mice and whether WT MSC transplant could also blunt this defect. The width between calcein green labels in the 8-day interim specifies the mineral apposition rate, which is used to calculate the bone formation rate (BFR) normalized to bone surface (BFR/BS) and bone volume (BFR/BV). Indeed, the BFRs (both BFR/BS and BFR/BV) were significantly impaired in naïve *Sca-1*^{-/-} mice versus WT controls (Fig. 4C, 4D). In contrast, *Sca-1*^{-/-} mice that received an MSC transplant displayed a significantly improved rate of bone formation (BFR/BS and BFR/BV; Fig. 4C, 4D).

Bone resorption is also perturbed in *Sca-1*^{-/-} mice because of an intrinsic osteoclast defect in addition to an inability of *Sca-1*^{-/-} osteoblasts to support osteoclast differentiation, leading to reduced osteoclast numbers and activity in vivo [25, 26]. Therefore, we next determined whether osteoclast number and surface area were improved in transplanted animals. *Sca-1*^{-/-} mice were transplanted as described above, and osteoclast number and surface area were assessed via tartrate-resistant acid phosphatase (TRAP) positive staining. Naïve *Sca-1*^{-/-} mice displayed significantly reduced bone surface occupied by osteoclasts (OcS/BS) and also a reduced number of osteoclasts on the bone surface (OcN/BS) compared with WT control mice (Fig. 4E, 4F). *Sca-1*^{-/-} mice transplanted with WT MSCs revealed significant improvement of OcS/BS (Fig. 4E) and OcN/BS (Fig. 4F).

The reduced bone turnover that occurs in osteoporosis leads to the highly mineralized, homogeneous, old bone, which we have observed in *Sca-1*^{-/-} mice [25, 26]. Quantitative backscatter electron imaging (BSE) was used to quantify the average mineral content (represented by Max Gray value) and assess full width at half-maximal height (FWHM) values, an indicator of mineral heterogeneity. Large FWHM values represent a heterogeneous mineralization profile of highly mineralized mature bone mixed with acutely mineralized matrix and new bone and are associated with higher bone turnover, whereas small FWHM values indicate the homogeneous, highly mineralized, old bone associated with low bone turnover. Six months after MSC

transplant, *Sca-1*^{-/-} treated mice had astonishingly high FWHM values (Fig. 4G). FWHM values in MSC-transplanted mice were nearly 200% above those observed for both WT and untreated *Sca-1*^{-/-} mice, indicating an exceptionally high level of bone turnover in MSC-transplanted mice.

Transplanted *Sca-1*^{-/-} Mice Displayed Improved Microarchitectural Characteristics

We sought to determine whether bone formation and quality gains observed in MSC-transplanted mice prevent the microarchitectural defects that occur in *Sca-1*^{-/-} mice [26]. The 10-week-old *Sca-1*^{-/-} mice were transplanted with 2×10^6 WT MSCs and assessed 24 weeks later, at 8.5 months of age, the time point when the osteopenic condition peaks in *Sca-1*^{-/-} mice [26]. Computed tomography (CT) is used clinically to identify microarchitectural aberrations in trabecular tissue associated with human aging and osteoporosis [36, 37]. Here, we performed microCT analyses on the proximal tibias of mice transplanted with WT MSCs, along with WT and naïve *Sca-1*^{-/-} controls. Trabecular connectivity-density (Conn.D), a measure of the interconnectivity of trabecular structures that provides strength to bone, displays a characteristic decline in osteoporosis [36]. *Sca-1*^{-/-} mice presented with significantly lower connectivity-density versus WT mice (Fig. 5A, 5G). However, *Sca-1*^{-/-} mice that received a single transplant of MSCs displayed significantly improved connectivity-density (Fig. 5A) and similar trabecular interactions to WT mice (Fig. 5G). Trabecular bone is highly anisotropic; thus, trabeculae are orientated preferentially in the direction of load bearing and exhibit a high degree of anisotropy (DA). Human aging and osteoporosis are hallmarked by decreased anisotropy [37].

Decreased anisotropy has been observed in another model of murine age-related osteoporosis [38], and we demonstrate herein a similar trend in the *Sca-1*^{-/-} mouse (Fig. 5B). Interestingly, *Sca-1*^{-/-} mice transplanted with WT MSCs demonstrated normal anisotropy (Fig. 5B).

Other clinically relevant osteopenic transformations present in the proximal tibia of *Sca-1*^{-/-} mice include decreased trabecular bone volume fraction (BV/TV), fewer trabecular structures (Tb.N), and an associated increased space between adjacent trabecular structures (Tb.Sp) (Fig. 5C–5E). Osteopenic increase in Structural Model Index (SMI) was also present in *Sca-1*^{-/-} mice and represents a progression toward weaker rod-shaped trabeculae in lieu of superior plate-like trabeculae (Fig. 5F). Specific statistical differences observed between WT and naïve *Sca-1*^{-/-} mice regarding BV/TV, Tb.N, Tb.Sp, and SMI were lost between WT and MSC-transplanted *Sca-1*^{-/-} mice, suggesting improvements in these metrics of osteoporosis (Fig. 5C–5F). Overall, microCT images of tibia of WT, untreated *Sca-1*^{-/-}, and MSC-transplanted *Sca-1*^{-/-} mice clearly reveal that transplanted animals present a trabecular structure similar to WT mice, with obvious improvements in connectivity (Fig. 5G).

DISCUSSION

Recent lineage tracing experiments have determined that within the MSC population, SSCs do indeed exist [15–18, 39]. Stem cells within the MSC population are required for long-term homeostasis, and their loss affects bone mass [18, 25]. Subsets of the MSC population can sense injury [40, 41] and effect repair and homeostasis through extensive clonal division, differentiation [18, 39],

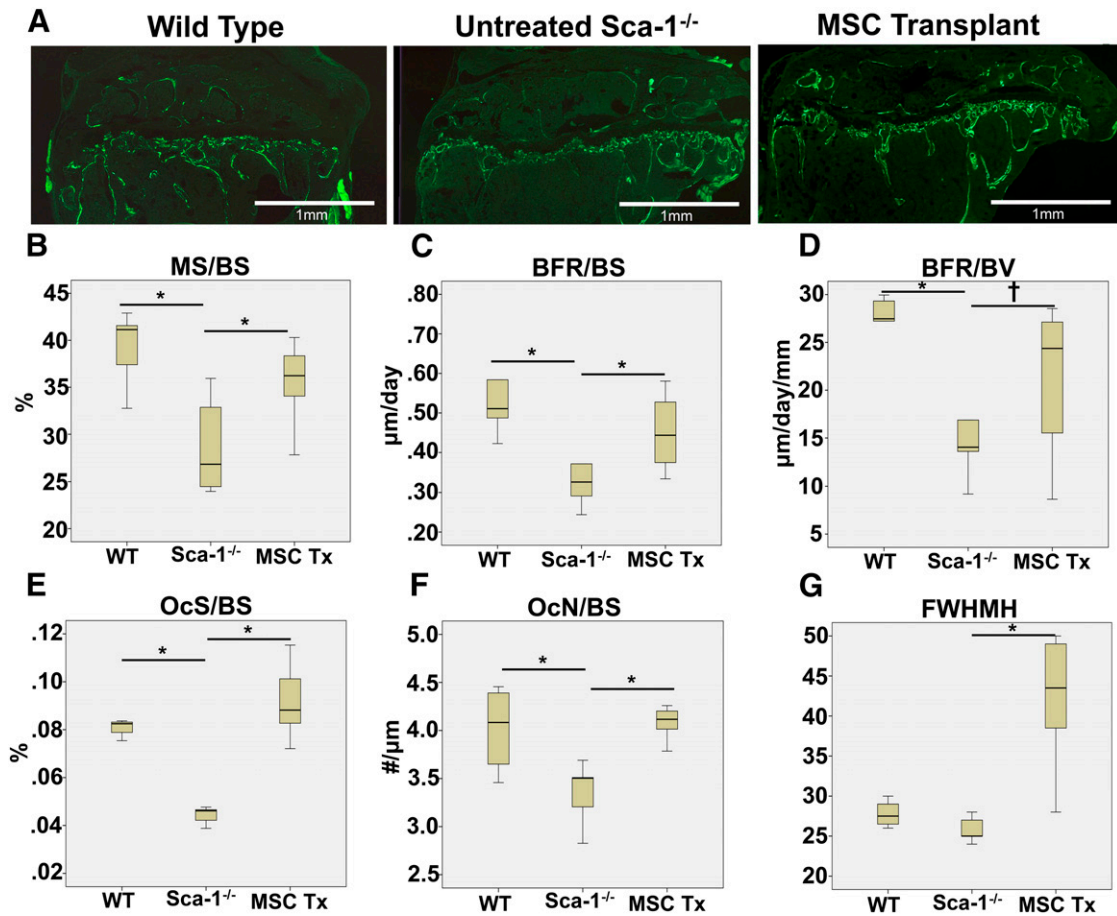


Figure 4. *Sca-1*^{-/-} mice that received a single MSC transplant display increased rate of bone formation, osteoclast activity, and bone turnover 6 months after transplant. **(A):** Representative fluorescent images of calcein staining in WT, naive *Sca-1*^{-/-}, and MSC-transplanted *Sca-1*^{-/-} mice. **(B):** Percent mineralizing surface normalized to bone surface. **(C):** Bone formation rate normalized to bone surface. **(D):** Bone formation rate normalized to bone volume. **(E):** Tartrate-resistant acid phosphatase (TRAP) analysis of osteoclast surface normalized to bone surface. **(F):** TRAP analysis of osteoclast number normalized to bone surface. **(G):** BSE imaging quantification of FWHMH, a measure of bone turnover. *, *p* ≤ .05; †0.1 ≥ *p* ≥ .05 [WT (*n* = 5 dynamic histo, *n* = 4 TRAP, BSE) *Sca-1*^{-/-} (*n* = 6 dynamic histo, TRAP, *n* = 5 BSE), MSC Tx (*n* = 8, all)]. Abbreviations: BFR/BS, bone formation rate normalized to bone surface; BFR/BV, bone formation rate normalized to bone volume; BSE, backscattered electron; FWHMH, full width at half-maximal height; MS/BS, percent mineralizing surface normalized to bone surface; MSC, mesenchymal stromal cell; MSC Tx, MSC-transplanted; OcN/BS, osteoclast number normalized to bone surface; OcS/BS, osteoclast surface normalized to bone surface; WT, wild type.

and paracrine effects [17, 42]. The findings that defective MSC self-renewal underlies age-related osteoporosis in a number of models suggest that MSCs, and by extension, SSCs within the heterogeneous population, are a potential therapeutic target for systemic skeletal diseases.

In this study, we determined that transplanted syngeneic MSCs led to persistent engraftment and improved bone formation and bone health in age-related osteopenic mice, at least 6 months after a single systemic injection. Additionally, improvements in bone homeostasis that resulted from maintaining tissue-resident MSCs further implicated the decline of MSCs associated with age-related osteoporosis as a major transformative event in the progression of the disease.

The *Sca-1*^{-/-} mouse is an ideal model of human age-related (type II) osteoporosis because, like the human condition, MSC defects cause an initial decrease in bone formation, which facilitates a reciprocal decrease in bone resorption, leading to a low-turnover state. This is in contrast to postmenopausal (type I) osteoporosis, which is driven by increased osteoclast activity

causing increased bone resorption that precipitates a high-turnover state. *Sca-1*^{-/-} mice display reduced bone formation [25], and trabeculae display higher mineralization with decreased turnover [26], characteristics confirmed in this study. *Sca-1*^{-/-} mice also exhibit reduced osteoclast numbers in vivo [25], also verified in this study. Together, reduced bone formation coupled with reduced osteoclast numbers and diminished bone turnover are indicative of fewer bone-remodeling cycles occurring in the *Sca-1*^{-/-} mice. These factors lead to older, highly mineralized bone, which, together with a reduction in overall bone, caused the mechanical weakness of trabecular tissue described previously [25, 26]. This model is consistent with human age-related osteoporosis, with a low-turnover state hallmarked by diminished and old, hypermineralized, mechanically inferior bone [9].

We have shown that WT MSC transplantation into *Sca-1*^{-/-} mice can indeed improve bone health. Remarkably, the *Sca-1*^{-/-} mice transplanted with a single bolus of MSC showed improved bone formation 24 weeks after transplantation. Likewise, bone

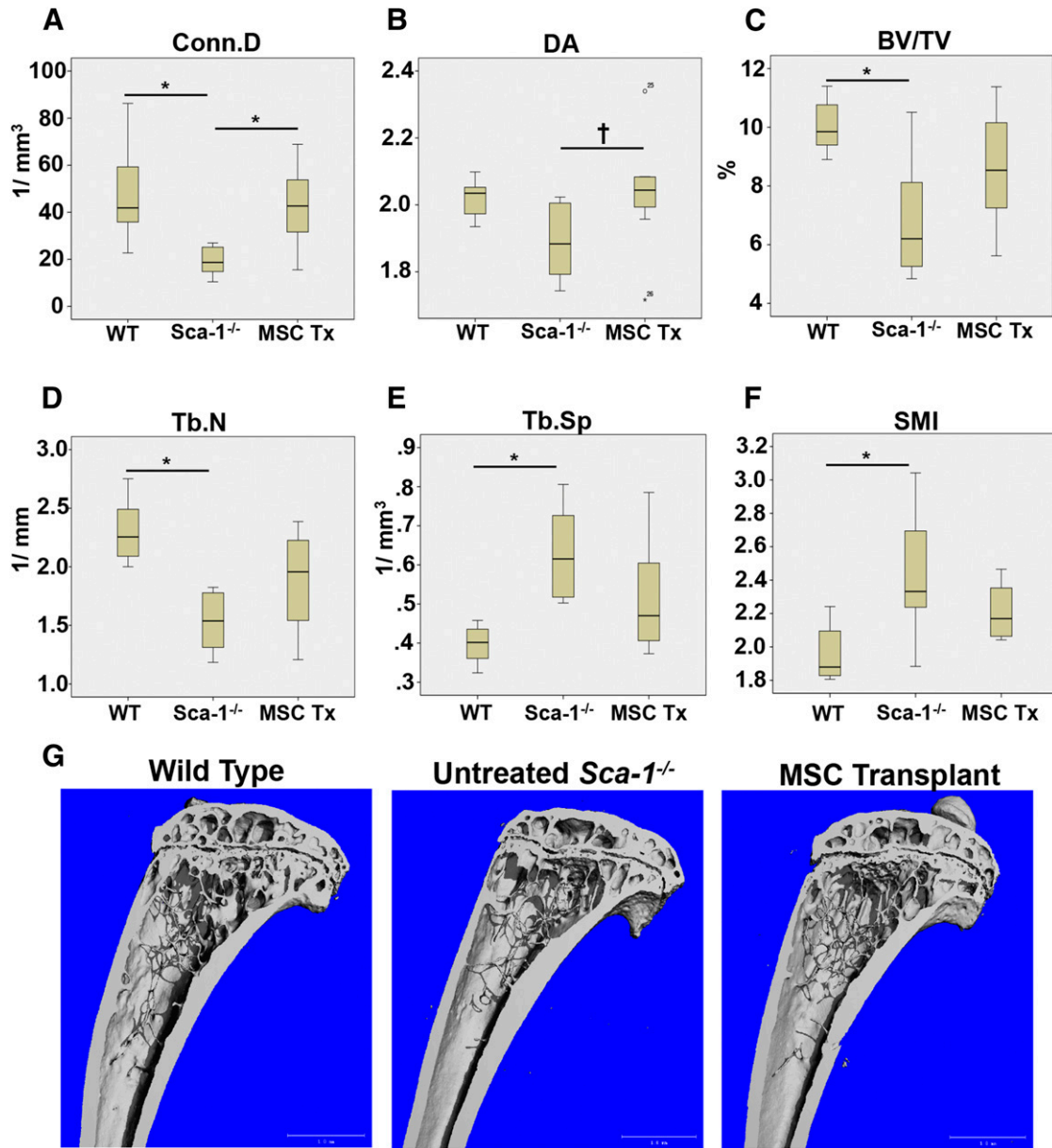


Figure 5. *Sca-1*^{-/-} mice that received a single MSC transplant display improved trabecular microarchitecture 6 months after transplant. MicroCT analysis of proximal tibias of WT, naïve *Sca-1*^{-/-}, and MSC-transplanted *Sca-1*^{-/-} mice (MSC Tx). Parameters investigated were as follows. (A): Connectivity density. (B): Degree of anisotropy. (C): Bone volume/total volume. (D): Trabecular number. (E): Trabecular spacing. (F): Structural Model Index. (G): Representative microCT images of WT, *Sca-1*^{-/-}, and MSC Tx mice. Scale bar = 1.0 mm. *, $p \leq .05$; †, $0.1 \geq p \geq .05$ [WT ($n = 7$), *Sca-1*^{-/-} ($n = 9$), and MSC Tx ($n = 8$)]. Abbreviations: BV/TV, bone volume/total volume; Conn.D, connectivity density; DA, degree of anisotropy; microCT, microcomputed tomography; MSC, mesenchymal stromal cell; MSC Tx, MSC-transplanted; SMI, Structural Model Index; Tb.N, trabecular number; Tb.Sp, trabecular spacing; WT, wild type.

catabolism was increased, leading to increased levels of bone turnover. These results together suggest that transplanted MSCs were capable of initiating or sustaining bone-remodeling cycles. This could be because of the ability of WT transplanted stromal cells to initiate and support osteoclast activity and/or the capacity of the transplanted WT MSCs to support bone formation itself. Old bone present in the low-turnover, age-related osteoporotic state accumulates microdamage, possibly reducing material toughness, and is hypermineralized, thereby increasing bone stiffness. Together, these changes may increase the likelihood of bone failure [9, 43, 44]. By restoring bone turnover in MSC-

transplanted animals, remodeling-mediated maintenance would return, allowing the resolution of microdamage and hypermineralization, potentially improving mechanical strength. However, the clinical relevance of microdamage and hypermineralization independently leading to increased fracture risk in humans remains controversial [43]. Mechanical testing of our MSC transplant system may be a good model to assess the mechanical and potentially clinical relevance of improved bone health, independent of anabolic bone growth.

It was also remarkable that one bolus of donor MSCs prevented age-related osteoporosis phenotypes as observed by

microCT 6 months after transplant. In human aging/osteoporosis, trabecular bone volume, number, and thickness decrease, whereas spacing increases [36, 45]. Anisotropy and connectivity decrease [36, 37], and SMI increases [46]. The *Sca-1*^{-/-} model of age-related osteoporosis displayed similar vertebral microarchitectural abnormalities [26], as does the *C57BL/6J* model of age-related osteoporosis [38]. Here we confirmed such microarchitectural aberrations at the metaphyseal tibial site.

Interestingly, transplanted *Sca-1*^{-/-} mice displayed complete protection from the phenotypic loss of connectivity and anisotropy, and partial protection from microarchitectural impairments of bone volume fraction, trabecular shape, number, and spacing. The mechanical integrity of trabecular bone is dependent on specific factors: bone volume, microarchitectural properties including connectivity and anisotropy, and matrix and mineral properties [27], all of which are affected in both human and *Sca-1*^{-/-} osteoporosis. First documented by D'Arcy Thompson in 1917, trabeculae maintain strength through connections with adjacent structures akin to girders in a high-rise building [1]. Loss of connectivity (lower Conn.D) represents disconnected trabeculae free floating within the medullary cavity, imparting no mechanical strength to the structure. It has been accepted, since the seminal treatise of Julius Wolff, that trabecular orientation is also important to mechanical strength—because of the anisotropic nature of cancellous bone—and that trabecular architecture is compromised in bony pathologies [2]. Remodeling results in preferential trabecular orientation in the direction of load bearing, which provides the requisite compressive resistance to ambulatory load. Loss of anisotropy (lower DA) represents a loss of trabecular resistance to load bearing, increasing the likelihood of compression fracture. Thus, the improved connectivity and the maintenance of anisotropy realized in transplanted animals represent potential improvement in bony mechanical strength and the restoration of a functional microarchitecture in MSC-treated *Sca-1*^{-/-} animals. Specifically, the change in trabecular bone volume observed in transplanted animals alone cannot explain this restoration in function because bone remodeling was also increased. However the increased trabecular remodeling, without significant changes in bone volume, resulted in microarchitectural improvements that, importantly, restored the wild-type structural anisotropic phenotype.

Indeed, we observed increased bone formation in transplanted animals, which seemed to contradict the modest improvements in bone volume observed by microCT. It is quite possible that improvements to overall bone formation in transplanted animals were being mitigated by the observed increased osteoclast activity. This increase in bone turnover was supported by the increase in the heterogeneity of mineral densities observed by backscatter electron photomicrography. Standard parathyroid (PTH) treatment for osteoporosis elicits a similar dynamic interaction between bone formation and resorption. Initial PTH-mediated bone formation gains are eventually mitigated by a reciprocal increase in resorption. The period where formation exceeds resorption defines the “anabolic widow” in which PTH treatment is most effective and usually lasts approximately 1 year [47]. To enlarge this anabolic window, combination therapy that includes bisphosphonates to decrease resorption is often recommended [48]. Thus, the use of bisphosphonates could potentially blunt the increased osteoclast activity observed after systemic MSC transplantation and realize more dramatic improvements in trabecular bone formation.

Transplanted MSCs are capable of long-term, albeit low-level, engraftment to endosteal bone and bone marrow in *Sca-1*^{-/-} mice, whereas engraftment in the lungs is three orders of magnitude higher than in the bone/bone marrow of recipient mice. Passive entrapment of donor cells within the vasculature cannot be ruled out because we did not determine whether the cells extravasated; however, the length of donor cell residency suggests engraftment. Murine bone marrow MSCs are exceedingly rare, with a frequency of 3 per million cells reported in BALB/c mice [32]; thus, comparable presence of donor MSCs within the recipient bone cellularity represents a significant contribution. Rare engraftment has been documented in other long-term MSC tracking studies that show similar therapeutic effect [49]. Potentially, donor MSCs could have differentiated into osteoblasts and subsequently matured into osteocytes. Osteocytes are known to survive for years within bone and are considered to play a major role in overall bone homeostasis [50]. Thus, a small number of donor-derived osteocytes could make significant contribution to relief of *Sca-1*^{-/-} osteopenia.

Donor MSCs were also detected in the lungs of recipient mice 24 weeks after transplant. Although not surprising that MSCs lodged within the lungs during short-term cell transplant experiments, it was interesting that they remained for an extended period of time. Transplanted MSCs in the lung are known to secrete therapeutic factors [33]. Thus, we cannot rule out the possibility that donor MSCs present in the lungs of *Sca-1*^{-/-} mice may contribute to the therapeutic effect that we observed; however, we demonstrated that secretion of M-CSF by lung MSCs does not underlie the observed increased osteoclastogenesis in transplanted mice. In addition, we investigated whether donor MSCs present in either the lung or bone marrow were acting via RANKL secretion to increase osteoclastogenesis. Interestingly, RANKL was not elevated in MSC-transplanted animals, suggesting another mechanism of action. However, RANKL is presented in both secreted and membrane-bound forms present on the surface of osteocytes and osteoblasts, with the latter displaying much higher osteoclastic activity [51]. Our analysis of transplanted mouse plasma could only detect the secreted form of RANKL; hence, upregulation of membrane-bound RANKL expression in treated animals could cause the increase in osteoclastogenesis.

Recently, it was found that a *Sca-1*-positive MSC population with a similar surface profile to the MSCs used in this study (*Sca-1*+*CD29*+*CD45*-*CD11b*-) is recruited to bone-remodeling sites, leading to bone formation. This action was mediated by the release of active transforming growth factor β (TGF- β) from bone by osteoclastic catabolism and was essential in coupling resorption to formation [52, 53]. *Sca-1* has been shown to suppress the accessibility of the TGF- β receptor complex to ligand binding [54]. Therefore, any TGF- β -mediated chemotaxis to sites of bone remodeling could be lost because of unabated TGF- β signaling in *Sca-1*^{-/-} MSCs, uncoupling the bone-remodeling process. Perhaps transplanted *Sca-1*+ MSCs were capable of proper recruitment to bone-remodeling sites, enabling proper initiation or maintenance of bone formation, or proper coupling with osteoclasts.

Aside from cytokine and growth factor-mediated paracrine effects elicited by MSCs, recent evidence suggests that MSCs can elicit effects through vesicle-mediated transport of various proteins and RNAs [55]. One particular study documented phenotypic correction of secondary osteoporosis in a murine model of lupus (Fas deficient *MLR/lpr* mice) via systemic WT MSC

transplant. The authors concluded that Fas was donated to the bone marrow MSCs of MLR/*lpr* MSCs through vesicle transfer, which initiated signaling events that improved long-term MLR/*lpr* bone marrow MSC function [56]. Sca-1 is a glycosylphosphatidylinositol-anchored lipid raft-associated protein that has been implicated in the disruption of broad Src kinase signaling [57], as well as inhibition of TGF- β [54] and peroxisome proliferator-activated receptor γ (PPAR γ) signaling [58]. We have previously observed high levels of Sca-1 protein within cell vesicles of wild-type mouse MSCs (J. Kiernan and W.L. Stanford, unpublished data). It will be interesting to test whether a similar mechanism occurs in our transplant model, with Sca-1 being transferred via vesicles from donor *Sca-1*^{+/+} MSCs to tissue-resident *Sca-1*^{-/-} MSCs (or other target cells) in transplanted mice, improving their function.

It has been demonstrated that culture expanded MSCs (both human and rodent) exhibit poor homing to the bone marrow [19], apparently because of large size [20] and inappropriate homing receptors [21, 59, 60]. In addition, efforts to modify the surface profile of MSCs to increase vascular attachment and homing have been reported, although it is unclear whether such strategies are amenable to clinical use [21, 60, 61]. Furthermore, our results demonstrate that such manipulation may not be necessary, and our minimally expanded MSCs (passage 1) highlight the utility of limited in vitro expansion.

CONCLUSION

As a first step to assess the capacity of MSCs to treat osteoporosis, we asked whether transplanted MSCs could maintain residence in the bone marrow long-term after intravenous transplantation and prevent the initiation of osteopenic pathologies in the *Sca-1*^{-/-} mouse model of age-related osteoporosis. We show that unmodified, low-passage MSCs are indeed capable of long-term bone marrow engraftment. The MSC-transplanted *Sca-1*^{-/-} mice demonstrated increased bone quality and normal trabecular connectivity and anisotropy, suggesting that low-level engraftment of a single bolus of MSCs is sufficient to blunt the development of osteopenic and osteoporotic phenotypes for at least 24 weeks. Given the numerous ongoing clinical trials utilizing

MSCs, we suggest that ancillary studies should be added to these clinical trials to determine whether transplantation of MSCs increase bone remodeling and improve bone health in the MSC-treated patients. These ancillary studies, or subsequent dedicated clinical trials, could determine whether age-related osteoporosis—a common, debilitating, and costly disease—could be treated by MSC transplantation. If MSC-mediated improvements in bone health and microarchitectural competence lead to fewer osteoporotic fractures in humans, this would emphasize clinical relevance of addressing bone health, turnover, and form, along with bone volume and density, in age-related osteoporosis treatment.

ACKNOWLEDGMENTS

We thank Drs. Christopher Yip, Bernhard Ganss, Andrey Shukalyuk, and Elnaz Ajami for helpful discussion. The research was supported by a training fellowship from the Canadian Institute of Health Research, Training Program in Regenerative Medicine (J.K.); Canadian Institutes of Health Research Grant FRN 62788 (to W.L.S.); and Natural Sciences and Engineering Research Council of Canada Grant RGPIN 293170-11 (to W.L.S.). W.L.S. is supported by the Canada Research Chair in Integrative Stem Cell Biology.

AUTHOR CONTRIBUTIONS

J.K.: conception and design, collection and/or assembly of data, data analysis and interpretation, manuscript writing; S.H. and M.D.G.: collection and/or assembly of data, data analysis and interpretation; J.E.D.: conception and design, data analysis and interpretation, manuscript writing; W.L.S.: conception and design, financial support, data analysis and interpretation, manuscript writing, final approval of manuscript.

DISCLOSURE OF POTENTIAL CONFLICTS OF INTEREST

The authors indicated no potential conflicts of interest.

REFERENCES

- 1 Thompson D. On Growth and Form. New York, NY: Macmillan Co., 1945:1116.
- 2 Wolff J. Das gesetz der transformation der knochen. Deutsche Medizinische Wochenschrift 1892;19:1222–1224.
- 3 Hodgskinson R, Currey J. The effect of variation in structure on the Young's modulus of cancellous bone: A comparison of human and non-human material. Proc Inst Mech Eng H 1990;204:115–121.
- 4 Goulet RW, Goldstein SA, Ciarelli MJ et al. The relationship between the structural and orthogonal compressive properties of trabecular bone. J Biomech 1994;27:375–389.
- 5 Manolagas SC, Parfitt AM. What old means to bone. Trends Endocrinol Metab 2010;21:369–374.
- 6 Leslie WD, Morin SN. Osteoporosis epidemiology 2013: Implications for diagnosis, risk assessment, and treatment. Curr Opin Rheumatol 2014;26:440–446.
- 7 Bellantuono I, Aldahmash A, Kassem M. Aging of marrow stromal (skeletal) stem cells and their contribution to age-related bone loss. Biochim Biophys Acta 2009;1792:364–370.
- 8 Muschler GF, Nitto H, Boehm CA, Easley KA. Age- and gender-related changes in the cellularity of human bone marrow and the prevalence of osteoblastic progenitors. J Orthop Res 2001;19:117–125.
- 9 Burr DB. Bone material properties and mineral matrix contributions to fracture risk or age in women and men. J Musculoskelet Neuronal Interact 2002;2:201–204.
- 10 Friedenstein AJ. Osteogenic stem cells in the bone marrow. In: Heersche JNM, Kanis JA, eds. Bone and Mineral Research. Amsterdam, The Netherlands: Elsevier Science Publishers, 1990.
- 11 Prockop DJ. "Stemness" does not explain the repair of many tissues by mesenchymal stem/multipotent stromal cells (MSCs). Clin Pharmacol Ther 2007;82:241–243.
- 12 Steinert AF, Rackwitz L, Gilbert F et al. Concise review: The clinical application of mesenchymal stem cells for musculoskeletal regeneration: current status and perspectives. STEM CELLS TRANSLATIONAL MEDICINE 2012;1:237–247.
- 13 Horwitz EM, Gordon PL, Koo WKK et al. Isolated allogeneic bone marrow-derived mesenchymal cells engraft and stimulate growth in children with osteogenesis imperfecta: Implications for cell therapy of bone. Proc Natl Acad Sci USA 2002;99:8932–8937.
- 14 Bianco P, Cao X, Frenette PS et al. The meaning, the sense and the significance: Translating the science of mesenchymal stem cells into medicine. Nat Med 2013;19:35–42.
- 15 Sacchetti B, Funari A, Michienzi S et al. Self-renewing osteoprogenitors in bone marrow sinusoids can organize a hematopoietic microenvironment. Cell 2007;131:324–336.
- 16 Méndez-Ferrer S, Michurina TV, Ferraro F et al. Mesenchymal and haematopoietic stem cells form a unique bone marrow niche. Nature 2010;466:829–834.
- 17 Chan CKF, Seo EY, Chen JY et al. Identification and specification of the mouse skeletal stem cell. Cell 2015;160:285–298.
- 18 Worthley DL, Churchill M, Compton JT et al. Gremlin 1 identifies a skeletal stem cell with bone, cartilage, and reticular stromal potential. Cell 2015;160:269–284.
- 19 Barbash IM, Chouraqui P, Baron J et al. Systemic delivery of bone marrow-derived mesenchymal stem cells to the infarcted

myocardium: Feasibility, cell migration, and body distribution. *Circulation* 2003;108:863–868.

20 Toma C, Wagner WR, Bowry S et al. Fate of culture-expanded mesenchymal stem cells in the microvasculature: In vivo observations of cell kinetics. *Circ Res* 2009;104:398–402.

21 Sackstein R, Merzaban JS, Cain DW et al. Ex vivo glycan engineering of CD44 programs human multipotent mesenchymal stromal cell trafficking to bone. *Nat Med* 2008;14:181–187.

22 Ichioka N, Inaba M, Kushida T et al. Prevention of senile osteoporosis in SAMP6 mice by intrabone marrow injection of allogeneic bone marrow cells. *STEM CELLS* 2002;20:542–551.

23 Cho SW, Sun HJ, Yang J-Y et al. Transplantation of mesenchymal stem cells overexpressing RANK-Fc or CXCR4 prevents bone loss in ovariectomized mice. *Mol Ther* 2009;17:1979–1987.

24 Guan M, Yao W, Liu R et al. Directing mesenchymal stem cells to bone to augment bone formation and increase bone mass. *Nat Med* 2012;18:456–462.

25 Bonyadi M, Waldman SD, Liu D et al. Mesenchymal progenitor self-renewal deficiency leads to age-dependent osteoporosis in Sca-1/Ly-6A null mice. *Proc Natl Acad Sci USA* 2003;100:5840–5845.

26 Holmes C, Khan TS, Owen C et al. Longitudinal analysis of mesenchymal progenitors and bone quality in the stem cell antigen-1-null osteoporotic mouse. *J Bone Miner Res* 2007;22:1373–1386.

27 Goldstein SA, Goulet R, McCubbrey D. Measurement and significance of three-dimensional architecture to the mechanical integrity of trabecular bone. *Calcif Tissue Int* 1993;53:S127–S132; discussion S132–S133.

28 Short BJ, Brouard N, Simmons PJ. Prospective isolation of mesenchymal stem cells from mouse compact bone. In: Audet J, Stanford WL, eds. *Stem Cells in Regenerative Medicine*. Totowa, NJ: Humana Press, 2009:259–268.

29 Cao X, Wu X, Frassica D et al. Irradiation induces bone injury by damaging bone marrow microenvironment for stem cells [published correction appears in *Proc Natl Acad Sci USA* 2011;108:5921]. *Proc Natl Acad Sci USA* 2011;108:1609–1614.

30 Wang H, Cao F, De A et al. Trafficking mesenchymal stem cell engraftment and differentiation in tumor-bearing mice by bioluminescence imaging. *STEM CELLS* 2009;27:1548–1558.

31 Cao Y-A, Wagers AJ, Beilhack A et al. Shifting foci of hematopoiesis during reconstitution from single stem cells. *Proc Natl Acad Sci USA* 2004;101:221–226.

32 Phinney DG, Kopen G, Isaacson RL et al. Plastic adherent stromal cells from the bone marrow of commonly used strains of inbred

mice: variations in yield, growth, and differentiation. *J Cell Biochem* 1999;72:570–585.

33 Lee RH, Pulin AA, Seo MJ et al. Intravenous hMSCs improve myocardial infarction in mice because cells embolized in lung are activated to secrete the anti-inflammatory protein TSG-6. *Cell Stem Cell* 2009;5:54–63.

34 Vedi S, Compston JE, Webb A et al. Histomorphometric analysis of dynamic parameters of trabecular bone formation in the iliac crest of normal British subjects. *Metab Bone Dis Relat Res* 1983–1984;5:69–74.

35 Arlot M, Edouard C, Meunier PJ et al. Impaired osteoblast function in osteoporosis: Comparison between calcium balance and dynamic histomorphometry. *Br Med J (Clin Res Ed)* 1984;289:517–520.

36 Hölzer A, Pietschmann MF, Rösl C et al. The interrelation of trabecular microstructural parameters of the greater tubercle measured for different species. *J Orthop Res* 2012;30:429–434.

37 Jiang Y, Zhao J, Liao E-Y et al. Application of micro-CT assessment of 3-D bone microstructure in preclinical and clinical studies. *J Bone Miner Metab* 2005;23(suppl):122–131.

38 Halloran BP, Ferguson VL, Simske SJ et al. Changes in bone structure and mass with advancing age in the male C57BL/6J mouse. *J Bone Miner Res* 2002;17:1044–1050.

39 Sarugaser R, Hanoun L, Keating A et al. Human mesenchymal stem cells self-renew and differentiate according to a deterministic hierarchy. *PLoS One* 2009;4:e6498.

40 Kark LR, Karp JM, Davies JE. Platelet releasate increases the proliferation and migration of bone marrow-derived cells cultured under osteogenic conditions. *Clin Oral Implants Res* 2006;17:321–327.

41 Karp JM, Tanaka TS, Zohar R et al. Thrombin mediated migration of osteogenic cells. *Bone* 2005;37:337–348.

42 Otsuru S, Gordon PL, Shimono K et al. Transplanted bone marrow mononuclear cells and MSCs impart clinical benefit to children with osteogenesis imperfecta through different mechanisms. *Blood* 2012;120:1933–1941.

43 Seref-Ferlenge Z, Kennedy OD, Schaffler MB. Bone microdamage, remodeling and bone fragility: How much damage is too much damage? *BoneKey Rep* 2015;4:644.

44 Turner CH. Biomechanics of bone: Determinants of skeletal fragility and bone quality. *Osteoporos Int* 2002;13:97–104.

45 Majumdar S, Genant HK, Grampp S et al. Correlation of trabecular bone structure with age, bone mineral density, and osteoporotic status: In vivo studies in the distal radius using high resolution magnetic resonance imaging. *J Bone Miner Res* 1997;12:111–118.

46 Ding M, Hvid I. Quantification of age-related changes in the structure model type and trabecular thickness of human tibial cancellous bone. *Bone* 2000;26:291–295.

47 Canalis E, Giustina A, Bilezikian JP. Mechanisms of anabolic therapies for osteoporosis. *N Engl J Med* 2007;357:905–916.

48 Cosman F. Anabolic and antiremodeling-mediated therapy for osteoporosis: Combination and sequential approaches. *Curr Osteoporos Rep* 2014;12:385–395.

49 Karp JM, Leng Teo GS. Mesenchymal stem cell homing: The devil is in the details. *Cell Stem Cell* 2009;4:206–216.

50 Bonewald LF. The amazing osteocyte. *J Bone Miner Res* 2011;26:229–238.

51 Nakashima T, Kobayashi Y, Yamasaki S et al. Protein expression and functional difference of membrane-bound and soluble receptor activator of NF-kappaB ligand: Modulation of the expression by osteotropic factors and cytokines. *Biochem Biophys Res Commun* 2000;275:768–775.

52 Wu X, Pang L, Lei W et al. Inhibition of Sca-1-positive skeletal stem cell recruitment by alendronate blunts the anabolic effects of parathyroid hormone on bone remodeling. *Cell Stem Cell* 2010;7:571–580.

53 Tang Y, Wu X, Lei W et al. TGF-beta1-induced migration of bone mesenchymal stem cells couples bone resorption with formation. *Nat Med* 2009;15:757–765.

54 Upadhyay G, Yin Y, Yuan H et al. Stem cell antigen-1 enhances tumorigenicity by disruption of growth differentiation factor-10 (GDF10)-dependent TGF-beta signaling. *Proc Natl Acad Sci USA* 2011;108:7820–7825.

55 Rani S, Ryan AE, Griffin MD et al. Mesenchymal stem cell-derived extracellular vesicles: Toward cell-free therapeutic applications. *Mol Ther* 2015;23:812–823.

56 Liu S, Liu D, Chen C et al. MSC transplantation improves osteopenia via epigenetic regulation of Notch signaling in lupus. *Cell Metab* 2015;22:606–618.

57 Holmes C, Stanford WL. Concise review: stem cell antigen-1: Expression, function, and enigma. *STEM CELLS* 2007;25:1339–1347.

58 Yuan H, Upadhyay G, Yin Y et al. Stem cell antigen-1 deficiency enhances the chemopreventive effect of peroxisome proliferator-activated receptor activation. *Cancer Prev Res (Phila)* 2012;5:51–60.

59 Wynn RF, Hart CA, Corradi-Perini C et al. A small proportion of mesenchymal stem cells strongly expresses functionally active CXCR4 receptor capable of promoting migration to bone marrow. *Blood* 2004;104:2643–2645.

60 Sarkar D, Spencer JA, Phillips JA et al. Engineered cell homing. *Blood* 2011;118:e184–e191.

61 Cheng Z, Ou L, Zhou X et al. Targeted migration of mesenchymal stem cells modified with CXCR4 gene to infarcted myocardium improves cardiac performance. *Mol Ther* 2008;16:571–579.



See www.StemCellsTM.com for supporting information available online.